

# Joining of AlN with metals and alloys

A. Kara-Slimane, D. Juve, E. Leblond, D. Treheux \*

*Laboratoire Ingénierie et Fonctionnalisation des Surfaces, UMR CNRS 5621, Ecole Centrale de Lyon, BP 163, 69131 Ecully Cedex, France*

Received 23 July 1999; received in revised form 3 January 2000; accepted 30 January 2000

---

## Abstract

The use of aluminium nitride in a wide range of applications depends on the capability to form strong AlN/AlN and AlN/metals (or alloys) joints. It has been shown that the different methods of joining, successfully used for alumina, solid-state bonding, liquid-state bonding and direct copper bonding (DCB, brazing), can be used for AlN. An optimisation of the different bonding parameters is required to obtain strong bonds. The influence of oxygen, nitrogen and the role of reactions products have been outlined. © 2000 Elsevier Science Ltd. All rights reserved.

*Keywords:* AlN; Bonding; Joining; Mechanical properties

---

## 1. Introduction

Aluminium nitride is a material more and more currently used instead of alumina for heat exchangers and heat engines because of both high thermal conductivity and high electrical resistivity. It is thus important to know the possibilities for making bonds between AlN and metals (or alloys) with the different technologies used for alumina up to date.

Joining of AlN has been the subject of some researches essentially focused on direct copper bonding technique (DCB)<sup>1,2</sup> and active metal brazing<sup>3–5</sup> which feasibility has been demonstrated.

This paper describes experiments on joining of AlN using, as examples, the solid state process with AlN/Cu (electronic applications) and AlN/Al/Steel (thermo-mechanical applications) and two liquid phase bonding processes: DCB (AlN/Cu) and brazing (AlN/Cu and AlN/Steel). The conditions required to obtain bonds of good quality, the interfacial chemistry and the influence of the different bonding parameters are discussed.

## 2. Experimental procedure

Blocks of commercial AlN ceramic with Y<sub>2</sub>O<sub>3</sub> (4 wt%) as sintering aid (C&C, Tarbes, France) were joined together or to stainless steel (Fe–17%wt Cr) with

either pure aluminium and copper (oxygen free high conductivity) foils as interlayer metals or Ag (72%wt)–Cu (28%wt) and Ag (62.94%wt)–Cu (35.4%wt)–Ti (1.66%wt) (CuSil ABA, WESGO-GTE) as commercial brazing alloys (0.1 mm thickness).

Shear or push-out test samples were fabricated in order to measure the fracture strength of the bonds (Fig. 1). In all cases, the fracture occurs in the elastic zone, the fracture strength corresponding to the maximum of the strain–deformation curve. Five measures have been carried out for each elaboration condition. Following mechanical testing, optical microscopy, scanning electron microscopy (SEM) observations, energy dispersive spectrometry (EDS) analyses and X-ray diffraction (conventional or grazing incidence) investigations were carried out in order to detect the presence of interfacial phases.

## 3. Solid state bonding

Whatever the materials used, bonds with high strength can be obtained providing an optimisation of the numerous processing parameters (time, temperature, applied pressure, radius/thickness ratio of the interlayer, friction at the interface related to the surface roughness of the ceramic). Thus is widely described in the literature, particularly for alumina.<sup>6–10</sup>

### 3.1. AlN/Cu/AlN

Bonds were elaborated using a copper foil (0.2 μm thick, 99.5% purity). AlN was polished and cleaned

---

\*Corresponding author.

E-mail address: dtreheux@ec-lyon.fr (D. Treheux).

with alcohol to an average surface roughness  $R_a$  of 0.2  $\mu\text{m}$ . Solid state bonding was performed in dynamic vacuum ( $5 \times 10^{-3}$  torr). Heating and cooling rates ranged from 150°C/h and 200°C/h. The influence of bonding time (2–5 h), temperature (1000–1050°C) and pressure (4 to 12 MPa) on the fracture strength is shown in Fig 2. The pressures leading to optimal strengths was 6 MPa for the two bonding times and temperatures investigated. This evolution is classically observed: the maximum correspond to the maximum bonding area and, for high pressure, the decrease is due to other mechanisms such as high shear stresses close to the interface and damage of materials (ceramic and metal) during bonding.<sup>6,11</sup>

All the fractures were adhesive (along the interface) when bonds were synthesised at 1000°C. GIXRD diffraction (Fig. 3) shows presence of AlN,  $\text{Al}_5\text{Y}_3\text{O}_{12}$  and Cu. Also,  $\text{Al}_2\text{O}_3$  and  $\text{CuAlO}_2$  were detected at interface probably due to AlN and copper oxidation. Thus suggested that the fracture occurs into the copper (near by the interfacial zone rich in reaction products  $\text{Al}_2\text{O}_3$ ,  $\text{CuAlO}_2$ ).

As a comparison, in similar experimental conditions (1000°C, 2 h, 6 MPa, primary vacuum), the Cu/ $\text{Al}_2\text{O}_3$

system are leading to mechanical resistance up to 80 MPa associated with cohesive fracture in alumina. It is due to Cu–O (clusters) interactions and a perfect matching of surfaces to be bonded (obtained 2 h after solid state bonding).<sup>8</sup> Consequently, the weakness of AlN/Cu bonds can be explained by difference of chemical bonding mechanisms: for  $\text{Al}_2\text{O}_3/\text{Cu}$ , copper-oxygen interactions are more important to strong adhesion.<sup>8</sup> In contrast, for AlN/Cu copper-aluminium interactions are more developed (11). Increasing both time and temperature (1050°C, 5 h), the strength slightly increases up to an applied pressure of 6 MPa where the maximum is reached (32 MPa), and then decreases (Fig. 2). The fracture becomes cohesive (in the bulk AlN) for 6 MPa. The increasing of mechanical behaviour at 1050°C is probably caused by migration of secondary phases at interfaces according results obtained for  $\text{Al}_2\text{O}_3/\text{Ni}$  system.<sup>7</sup>

### 3.2. AlN/Al/Steel bonding

When aluminium is used as interlayer, the bonding pressure must be high (10 MPa) to break the superficial

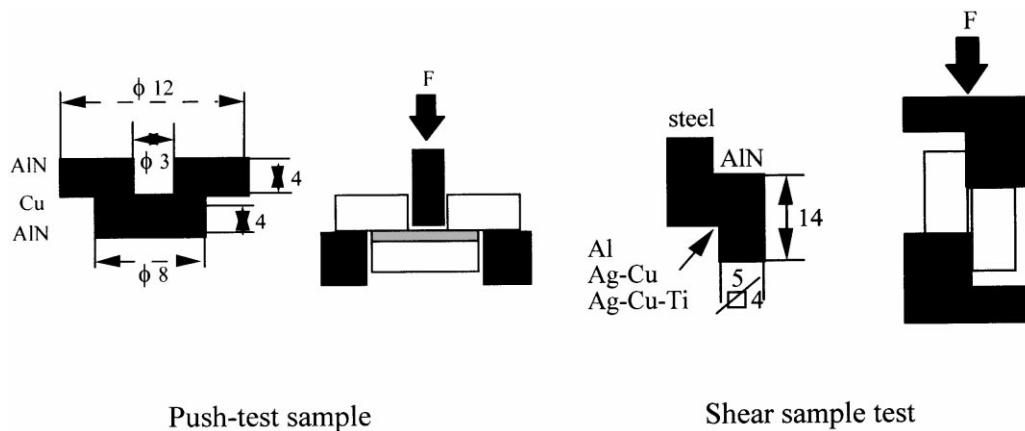


Fig. 1. Samples and mechanical tests used (loading rate 0.1 mm/mn).

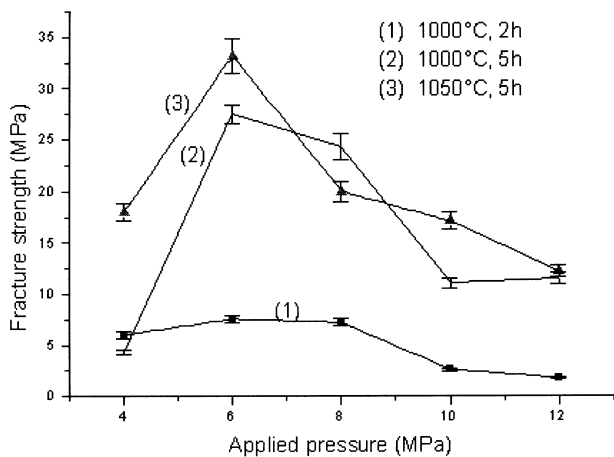


Fig. 2. Push-test bonding strength vs. applied pressure for AlN/Cu joint obtained by solid state bonding at  $5 \times 10^{-3}$  torr vacuum.

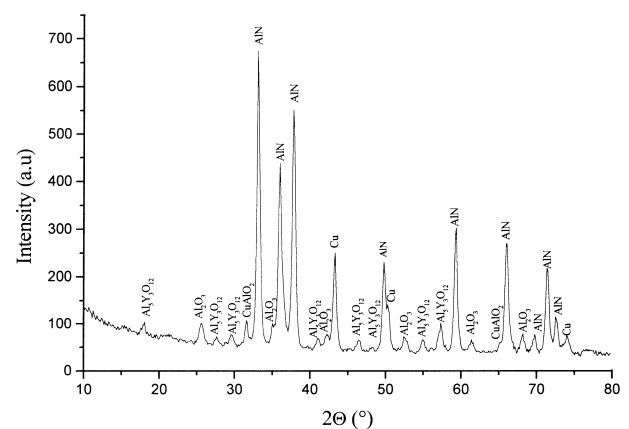


Fig. 3. GIXRD spectrum ( $\text{Cu } K_{\alpha}$ ) of the fracture surface (AlN side) of the AlN/Cu/AlN solid state bonding ( $T=1000^{\circ}\text{C}$ ,  $5 \times 10^{-3}$  torr vacuum,  $t=2$  h,  $P=6$  MPa).

alumina layer always present and to ensure a true contact between aluminium and the material to be bonded.<sup>12</sup> Joints were elaborated using Al foil of 0.2 mm thickness.

The influence of the bonding temperature (600–650°C) on the fracture strength, measured by shearing, has been investigated for two bonding time plateau (0–2 h) (Fig.4). The pressure is continuously applied during the bonding cycle. Whatever the temperature, a short bonding time gives strongest bonds. If the bonding time is raised, the fracture strength decreased to no adherence. Micrographic observations (Fig. 5) and X-ray diffraction spectrum (Fig. 6) shows that intermetallic phase identified as Fe<sub>2</sub>Al<sub>5</sub> grows between aluminium and steel at any bonding temperature and time. Thus upon testing, for long bonding time cracks preferentially propagated in the brittle compound Fe<sub>2</sub>Al<sub>5</sub> as shown by XRD diffraction patterns performed on the two sides failure surfaces (Fig. 6). The strength of the bond is directly associated to the Fe<sub>2</sub>Al<sub>5</sub> thickness: as the Fe<sub>2</sub>Al<sub>5</sub> layer increases, the bond degrades (Fig. 7). For short

bonding time the fracture propagated at Al/AlN interface and the fracture strength is 50–60 MPa (Fig. 7).

#### 4. Liquid state bonding

Liquid metals do not wet alumina nor aluminium nitride.<sup>8</sup> Based on works of Rhee,<sup>5</sup> the contact angle of

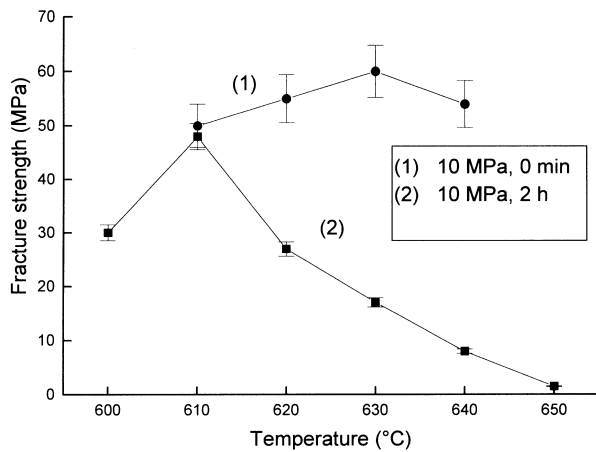


Fig. 4. Shear strength vs. bonding temperature for AlN/Al/steel joint (solid state bonding  $P=10$  MPa,  $5 \times 10^{-3}$  torr vacuum).

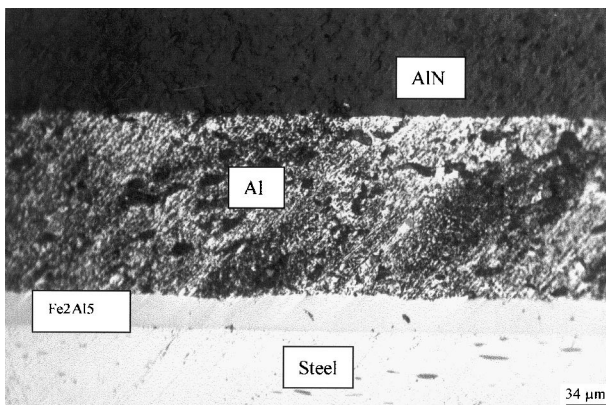


Fig. 5. Optical micrography of an AlN/Al/steel joint solid state bonded at 630°C for 0 mm and 10 MPa,  $5 \times 10^{-3}$  torr vacuum.

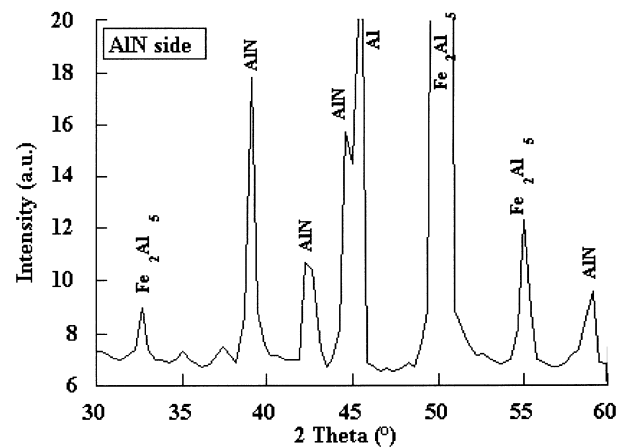
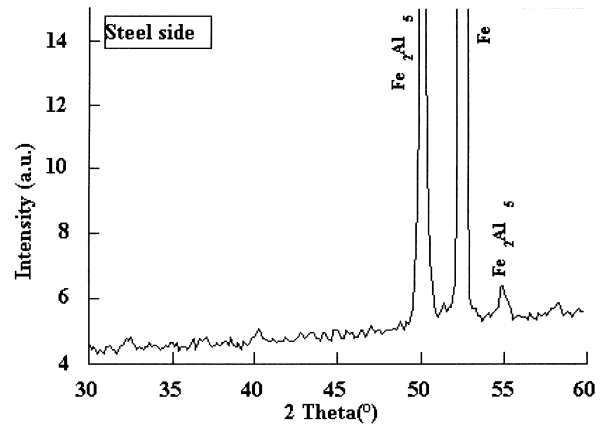


Fig. 6. X-ray diffraction spectrum (Cu  $K_{\alpha}$ ) of the fracture surface of AlN/Al/Steel joint in the conditions: 10 MPa, 620°C, 2 h.

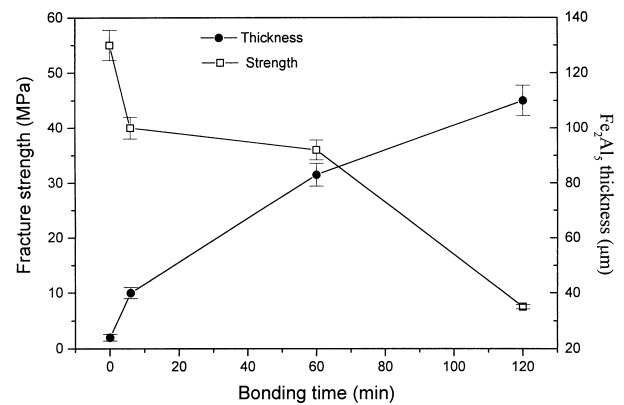


Fig. 7. Evolution of the bond strength (shear test) of the AlN/Al/steel vs thickness of Fe<sub>2</sub>Al<sub>5</sub> (bonding conditions: 640°C, 10 MPa).

copper on AlN surface at 1100°C was 147° and the one silver at 1000°C was 152°. Consequently, to enhance the wettability intermediary phases or active metals are needed (as for alumina) for bonding.<sup>3,8,13</sup>

#### 4.1. Direct copper bonding

DCB technique is based on the presence of an eutectic between copper and Cu<sub>2</sub>O (0.39 wt% O<sub>2</sub>, T<sub>m</sub> = 1065°C) which wets alumina. The process can thus be successfully used only if the AlN surface is oxidised in alumina, in air or in an oxygen atmosphere.<sup>1,2</sup> AlN was held at 1200°C in air for 1 to 180 min to obtain various thickness of the alumina layer. Copper was also oxidised at 1000°C before bonding. The two oxidised materials were thus pressed together and held at 1070°C (below 1083°C, melting point of copper and above the melting point of eutectic) during 1–2 min. Then, the eutectic phase was appeared and brought the copper in intimate contact with AlN by wetting and reacting with alumina to form the binary oxide CuAlO<sub>2</sub>.<sup>11,13</sup>

The composition of the bonding atmosphere is very important since the initial Cu<sub>2</sub>O must be maintained. If the oxygen partial pressure is too high, all copper is

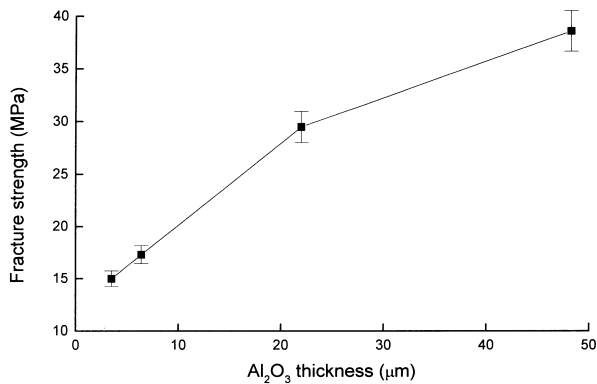


Fig. 8. Influence of Al<sub>2</sub>O<sub>3</sub> thickness on the bonding strength push-test of AlN DCB (1073°C, 4 mm, Cu<sub>2</sub>O thickness = 0.87 μm, atmosphere: Ar + 70 ppm O<sub>2</sub>).

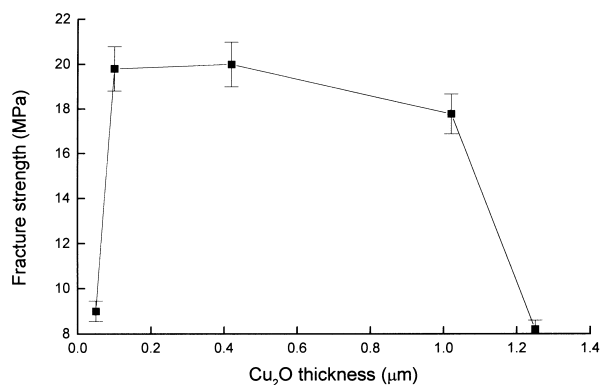


Fig. 9. Influence of Cu<sub>2</sub>O thickness on the bonding strength shear test of AlN DCB (1073°C, 6 mm, Al<sub>2</sub>O<sub>3</sub> thickness = 4.7 μm, Ar + 70 ppm O<sub>2</sub>).

converted into eutectic melt, conversely if the partial pressure is less than the equilibrium partial pressure over Cu<sub>2</sub>O at 1065°C (1.1 10<sup>-3</sup> torr), oxide is reduced and the eutectic phase will not form. The trends in fracture strength of AlN/AlN bonds measured as a function of alumina and Cu<sub>2</sub>O thickness (measured by microscopy) are given respectively in Figs. 8 and 9 for bonding performed in argon with 70 ppm O<sub>2</sub>.

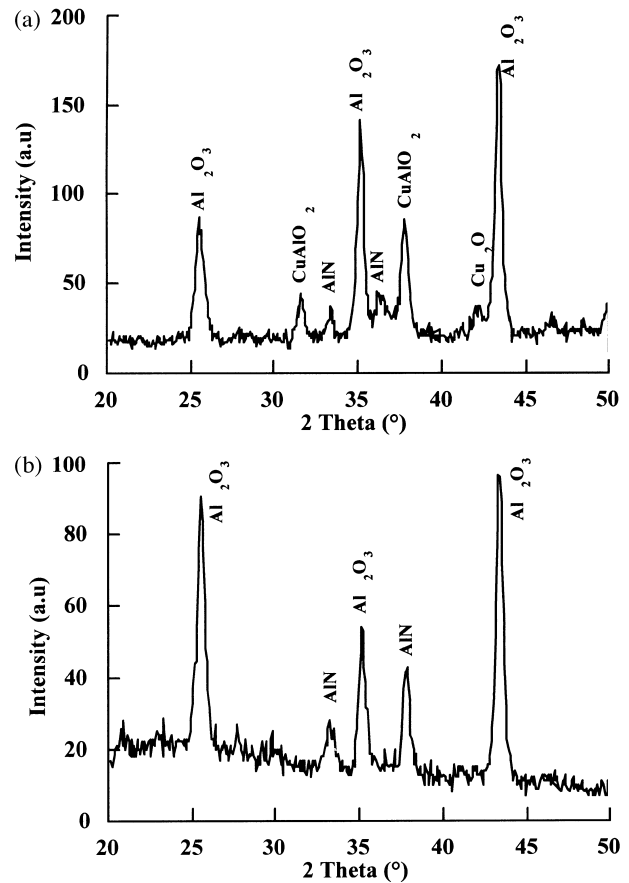


Fig. 10. Grazing X-ray diffraction spectrum (Cu K<sub>α</sub>) of the fracture surface of AlN: (a) push-test strength = 1 MPa, (b) push-test strength = 40 MPa.

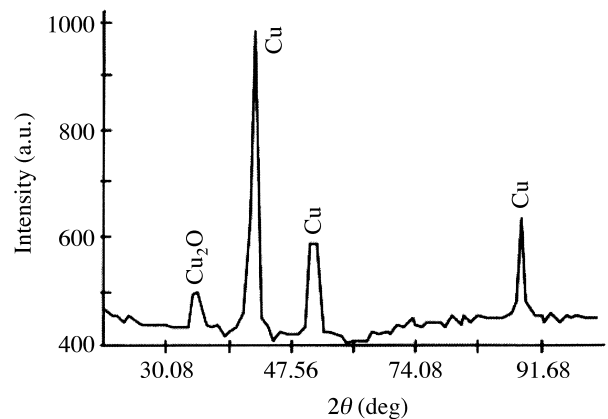


Fig. 11. Grazing X-ray diffraction spectrum (Cu K<sub>α</sub>) of the as-sprayed copper deposit on AlN ceramic.

The bond strength always increases with the alumina thickness (Fig 8) (up to 50  $\mu\text{m}$ , maximum value investigated). On the contrary, varying the  $\text{Cu}_2\text{O}$  thickness, the strength first increases up to 0.2  $\mu\text{m}$  where the maximum reaches and maintains over the range 0.2–0.5  $\mu\text{m}$ , then it decreases to zero for 1.2  $\mu\text{m}$  (Fig. 9). In fact, thin  $\text{Cu}_2\text{O}$  layers (<0.1  $\mu\text{m}$ ) are associated with small amounts of eutectic, thus to local bonding. Increasing

the  $\text{Cu}_2\text{O}$  layer enabled the eutectic to form and therefore to wet the entire AlN surface. But if the  $\text{Cu}_2\text{O}$  thickness is too high (>0.5  $\mu\text{m}$ )  $\text{Cu}_2\text{O}$  are not always entirely converted into eutectic melt and consequently, on testing, cracks develop along the residual  $\text{Cu}_2\text{O}/\text{CuAlO}_2$  interface, as shown by X-ray diffraction experiments made on the fracture surface (Fig. 10a). On the contrary, in the range 0.2–0.5  $\mu\text{m}$ , all the  $\text{Cu}_2\text{O}$

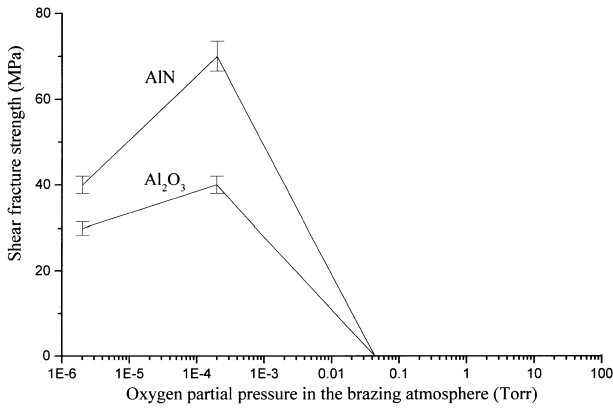


Fig. 12. Influence of the brazing atmosphere on the shear strength of AlN/AgCu/Cu and Al<sub>2</sub>O<sub>3</sub>/AgCu/Cu<sup>8</sup> bonds ( $T=820^\circ\text{C}$ ,  $t=1$  min).

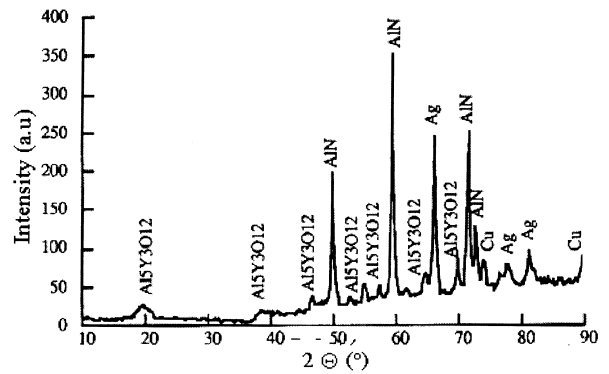


Fig. 13. GIXRD spectrum ( $\text{Cu } K_\alpha$ ) of the fracture surface (AlN side) of the AlN/AgCu/Cu assembly brazed at  $820^\circ\text{C}$ ,  $t=1$  mm  $P_{O_2} = 2 \times 10^{-4}$

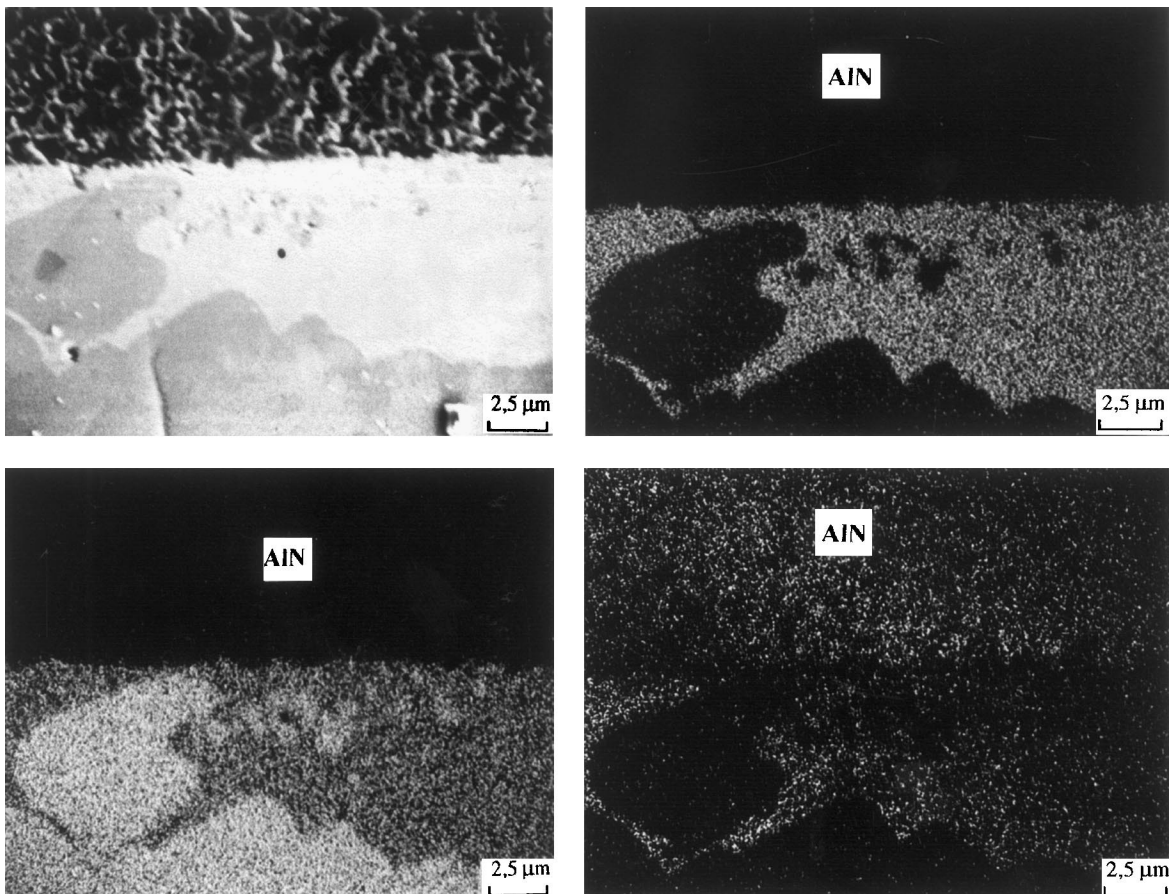


Fig. 14. WDX analysis of AlN/AgCu/Cu assembly brazed in primary vacuum at  $820^\circ\text{C}$ ,  $t=1$  min.

reacts to form binary oxide  $\text{CuAlO}_2$ . In this case, according to the good plasticity of  $\text{CuAlO}_2$ ,<sup>16</sup> bonds are stronger and the fracture appears in the  $\text{AlN}/\text{Al}_2\text{O}_3$  interphase (Fig. 10b).

#### 4.2. Non-reactive brazing $\text{AlN}/\text{Cu}$

The composition of the brazing alloy was Ag72–Cu 28 wt%. Brazing was performed at 820°C, 1 min in either vacuum or air. As with alumina,<sup>8</sup> the braze does not wet  $\text{AlN}$ . Consequently, before bonding,  $\text{AlN}$  surface was plasma-sprayed by copper powders in air as previously used for  $\text{Al}_2\text{O}_3/\text{Cu}$  brazing.<sup>8</sup> Plasma spraying of copper on  $\text{AlN}$  leads to the formation of a composite layer (20–40  $\mu\text{m}$  thick) constituting of Cu and  $\text{Cu}_2\text{O}$  as shown by X-ray diffraction (Fig. 11).

As for  $\text{Al}_2\text{O}_3/\text{Cu}$  system,<sup>8</sup> the shear strength observed for as-sprayed  $\text{AlN}/\text{copper}$  bonds is strongly affected by the oxygen partial pressure in the brazing atmosphere (Fig. 12).

Stronger bonds are obtained for  $2 \times 10^{-4}$  torr  $P_{\text{O}_2}$  atmosphere. The strength decreases for higher or lower  $P_{\text{O}_2}$ . GIXRD analysis (Fig. 13) did not detect any new phases but only copper, silver and  $\text{AlN}$  associated to secondary phase  $\text{Al}_5\text{Y}_3\text{O}_{12}$ .  $\text{Cu}_2\text{O}$  (present before brazing) and  $\text{CuAlO}_2$  were not detected after bonding.

These results are in good agreement with alumina joined in the same conditions but with shear fracture strength higher with  $\text{AlN}$  than alumina (70 against 40 MPa for alumina).

WDX maps (Fig. 14) of the cross-sections of the optimal sample shows that aluminium, associated with silver, diffuses in the brazing alloy through the initial copper deposit. Those results suggested that  $\text{AlN}$  in contact with the metallic melt decompose during brazing to form Ag–Al liquid solution. This is in good agreement with silver–aluminium phase diagram.<sup>17</sup> Also, copper oxide  $\text{Cu}_2\text{O}$  present in the pre-sprayed layer decomposes to make oxygen available for the good wetting of ceramic. Such an hypothesis is consistent with other results that clearly show the critical role of oxygen to enhance wetting and reactions in several systems such as  $\text{Al}_2\text{O}_3/\text{Cu}$ ,<sup>4,11</sup> and  $\text{Al}_2\text{O}_3/\text{Ag}$ .<sup>9</sup> Furthermore, the presence of  $\text{Al}_5\text{Y}_3\text{O}_{12}$  at the interface can be traduced the formation either by capillarity from the grains boundary of  $\text{AlN}$  as for  $\text{Ni}/\text{Al}_2\text{O}_3$ <sup>7</sup> and  $\text{Pt}/\text{Al}_2\text{O}_3$ <sup>18</sup> or by reaction due to decomposition of  $\text{AlN}$  and residual oxygen.

Indeed, depending on oxygen content, present both in the atmosphere and copper metallisation, is likely an oxinitride layer  $\text{AlN}_x\text{O}_y$  onto  $\text{AlN}$  surface at 820°C.<sup>19</sup> Thus, are similar conditions described for  $\text{AlN}$  support this assumption.

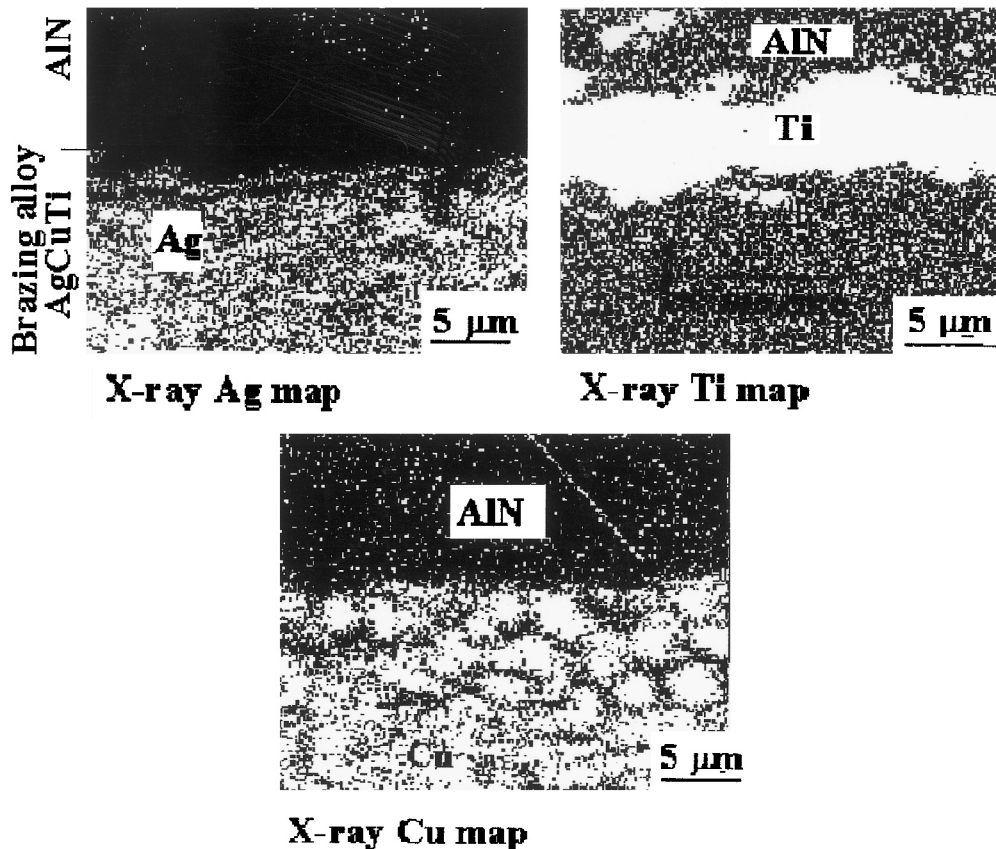


Fig. 15. WDX analysis of  $\text{AlN}/\text{AgCuTi}/\text{steel}$  assembly brazed at 850°C,  $t = 5$  min and  $P_{\text{O}_2} = 2 \times 10^{-4}$  torr.

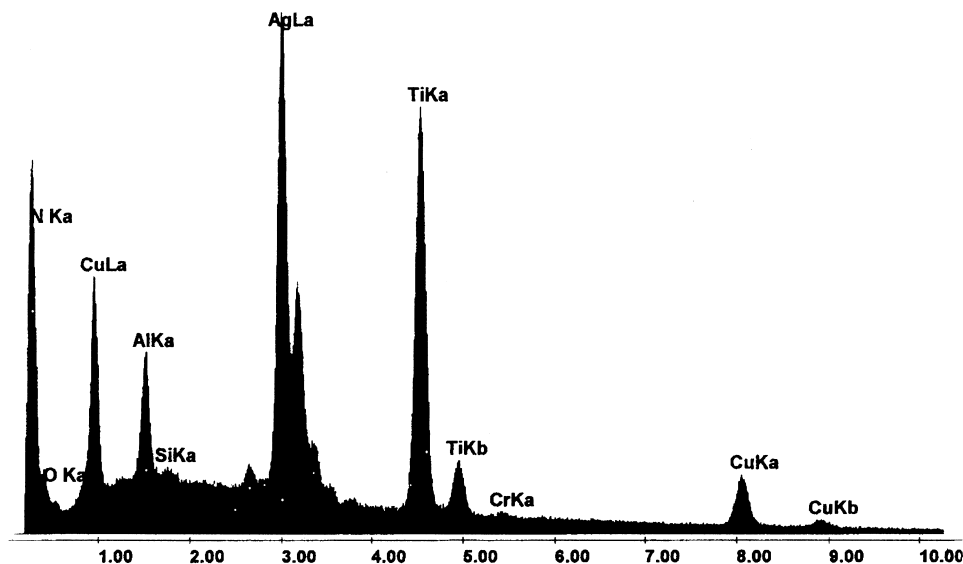


Fig. 16. EDS analysis of the AlN/AgCuTi/steel assembly near the MN/brazing alloy interface ( $T=850^{\circ}\text{C}$ ,  $t=5$  min,  $P_{\text{O}_2} = 2 \times 10^{-4}$  torr).

#### 4.3. Reactive brazing AlN/Steel

AlN was joined to steel using a conventional braze alloy (CuSil ABA) with the following composition: Ag 62.95–Cu 35.4–Ti 1.66 wt%. Bonding was achieved at  $850^{\circ}\text{C}$  for 5 min under primary vacuum.<sup>11</sup> The fracture happens in the ceramic bulk and the shear fracture strength was 50 MPa.

Titanium containing alloys react rapidly with AlN. WDX observations (Fig. 15) indicate that titanium segregates at the AlN/brazing alloy interface to form titanium nitride TiN as proved both by EDS analysis (Fig. 16) and XRD diffraction. The proposed mechanism is decomposition of AlN associated with aluminium and nitrogen diffusion into the brazing alloy. This reaction product has a primordial role for mechanical properties of interface.<sup>20</sup>

It is interesting that for  $\text{Al}_2\text{O}_3$ /steel system, elaborated in the same conditions, lower fracture strength (38 MPa) were observed. XRD diffraction detects TiO phase at

the interface (Fig. 17) instead of TiN for AlN/steel. Also, TiN phase accommodates internal stresses because thermal expansion mismatches AlN and steel<sup>21</sup> during cooling.

#### 5. Conclusions

Classical processes used for metal/ceramic bonding can be transposed for AlN/metal systems with the same precaution concerning the formation of reaction products which nature and morphology have been optimised.

For Cu/AlN system, oxygen reacts as reactive element either by oxidation of AlN, forming  $\text{Al}_2\text{O}_3$  or/and by copper oxidation. Afterwards the classical reaction between  $\text{Al}_2\text{O}_3$  and  $\text{Cu}_2\text{O}$  leading to  $\text{CuAlO}_2$  take place. Whatever the process solid-state bonding or liquid state bonding, the best results were obtained for an optimal thickness of  $\text{CuAlO}_2$  and  $\text{Al}_2\text{O}_3$  which dictates strict joining conditions, especially for oxygen content in metal and bonding atmosphere. However for this system, pre-metallisation of AlN by atmospheric plasma spraying permit to elaborate strong AlN/Cu bonds using classical AgCu non-reactive brazing alloy. Such excellent results were linked up to aluminium diffusion through brazing alloy without formation of reactions products. Once more, oxygen present in pre-metallisation layer or bonding atmosphere seems to play a significant role.

Titanium addition, in AgCu filler alloy, totally modify the bonding mechanism because titanium segregates at the AlN interface and reacts with AlN to form TiN.

Finally, the AlN/Al/steel system reveals the necessity to control all the reaction products growing during bonding. Indeed the AlN/Al interface is non-reactive system and to Al/steel is reactive interface leading to the intermetallic  $\text{Fe}_2\text{Al}_5$  compound, which is particularly brittle.

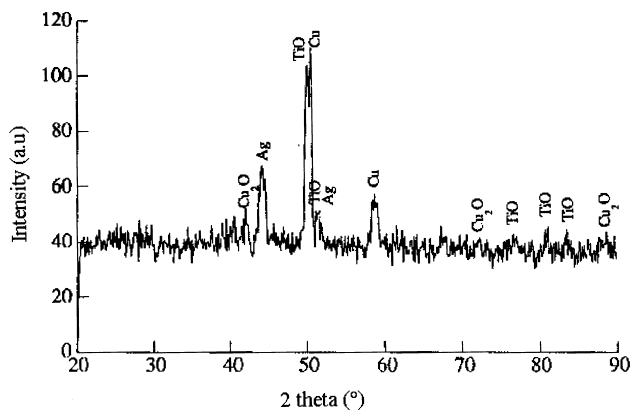


Fig. 17. XRD spectrum ( $\text{Cu K}_\alpha$ ) of the fracture surface (alumina side) of  $\text{Al}_2\text{O}_3$ /AgCuTi/steel bonding brazed at  $850^{\circ}\text{C}$ ,  $P_{\text{O}_2} = 2 \times 10^{-4}$  torr,  $t=5$  mm.

## References

1. Kluge-Weiss, P. and Gobrecht, J., Directly bonded metallization of AlN substrates for power hybrids. *Mater. Res. Soc. Symp. Proc.*, 1985, **40**, 399–404.
2. Guinet, J. and Michelet, J. P., Méallisation directe de cuivre sur substrats nitrures d'aluminium. In *Intern. Conf. on. Microelect. Hybrid.*, Rotterdam, 1991.
3. Carim, A. and Loehman, R. E., Microstructure at the interface between AlN and a Ag–Cu–Ti braze alloy. *J. Mater. Res.*, 1990, **5**, 1520–1529.
4. Ohuchi, F. S., In *Metal–Ceramic Interfaces* M. Rühle and A. G. Evans. Pergamon Press, 1990.
5. Rhee, S. K., Wetting of AlN and TiC by liquid Ag and liquid Cu. *J. Am. Ceram. Soc.*, 1970, **53**, 639–641.
6. Tréheux, D., Lourdin, P., Mbongo, B. and Juvé, D., Metal–ceramic solid state bonding: mechanisms and mechanics. *Scripta Metall. Mater.*, 1994, **31**, 1055–1060.
7. Lourdin, P., Juvé, D. and Tréheux, D., Nickel–alumina bonds: mechanical properties related to interfacial chemistry. *J. Eur. Ceram. Soc.*, 1996, **16**, 745–752.
8. Kara-Slimane, A., Mbongo, B. and Treheux, D., Adhesion and reactivity in the copper-alumina system: influence of oxygen and silver. *J. Adh. Sci. Tech.*, 1999, **13**, 35–48.
9. Serier, B. and Treheux, D., Silver–alumina solid state bonding: influence of the work hardening of the metal. *Acta. Metall. Mater.*, 1993, **41**, 369–374.
10. Mbongo, B., Thesis, ECL 94-30, 1994.
11. Tréheux, D., Lourdin, P., Guipont, V. and Juvé, D., Mechanical behaviour of metal–ceramic bonds. *J. Phys III*, 1994, **4**, 1883–1898.
12. Klomp, J. T., Solid state bonding of metals to ceramics. *Science of ceramics*, 1970, **5**, 501–522.
13. Leblond, E. DEA report, Ecole Centrale de Lyon, 1994
14. Gallois, B., Contribution to the physical chemistry of metal-gas and metal-Al<sub>2</sub>O<sub>3</sub> interface. Thesis, Carnegie Mellon University, Pittsburgh E.U., 1980.
15. Ohushi, F.S., French, R.H. Effect of oxygen incorporation in AlN thin films. *J. Sci. Technol.*, 1987, 1695–1696.
16. Berraud, C., Esnouf, C., Courbière, M., Juvé, D. and Tréheux, D., Bonding structure and mechanical properties of Cu–Al<sub>2</sub>O<sub>3</sub>. *J. Mater. Sci.*, 1989, **24**, 4545–4554.
17. Hansen, H., Anderko, K., *Constitution of Binary Alloys*. Mac-Graw–Hill Co. New York, (1958).
18. Dalfeish, B. J., Saiz, E., Tomsia, A. P., Cannon, R. M. and Ritchie, R. O., Interface formation and strength in ceramic-metal systems.. *Scripta. Metall. Mater.*, 1994, **31**, 1109–1114.
19. Khan, A. A. and Labbe, J. C., Alumminium Nitride–molybdenum ceramic matrix composites characterization of ceramic–metal interface. *J. Eur. Ceram. Soc.*, 1996, **16**, 739–744.
20. Tanaka, T., Hoomma, H. and Morimoto, H., Joining of ceramic to metals. *Nippon Steel Technical Report*, 1988, **37**, 31.
21. Tomsia, A.P., Saiz, E., Foppiano, S. and Cannon, R. M. Reactive wetting in ceramic/metal system. In *Proceed. of the World Ceramics Congress, 9th CIMTEC*, 1998, pp. 913–926